

# Structural member stability verification in the new Part 1-1 of the second generation of Eurocode 3

## Part 2: Member buckling design rules and further innovations

This two-part article gives an overview of the developments of the structural member verification in prEN 1993-1-1:2020 “Eurocode 3: Design of steel structures – part 1-1: General rules and rules for buildings”, one of the second generation of Eurocodes. These developments were undertaken by Working Group 1 (WG1) of Subcommittee CEN/TC250/SC3 and by Project Team 1 (SC3.PT1) responsible for drafting the new version of EN 1993-1-1. In the past, WG1 collected many topics needing improvement, and the systematic review conducted every five years also yielded topics needing further development. Based on this, the current version of EN 1993-1-1 has been developed into a new draft version prEN 1993-1-1:2020 enhancing “ease of use”. The technical content of this new draft was laid down at the end of 2019. Many improvements to design rules have been established with respect to structural analysis, resistance of cross-sections and stability of members. This two-part article focuses on member stability design rules and deals with the basis for the calibration of partial factors, the introduction of more economic design rules for semi-compact sections, methods for structural analysis in relation to the appropriate member stability design rules, new design rules for lateral torsional buckling plus other developments and innovations. This second part of the article is dedicated to illustrating the most relevant changes to member buckling design rules.

**Keywords** steel structures; structural stability; Eurocode 3; standardization; flexural buckling; lateral torsional buckling; cross-sectional capacity

### 1 Introduction to and scope of the second part of the article

The first part of this article, published in the preceding issue of this journal, was mostly dedicated to the general background to European Commission Mandate M/515 [1] for the evolution of the Eurocodes and to the changes in prEN1993-1-1:2020 that concern material grades, partial factors, cross-sectional classification and checks as well as structural analyses. Continuing the illustration of the background to the changes and innovations contained in prEN1993-1-1:2020, this second part of the article is mostly dedicated to the developments pertaining to member buckling design rules. In section 2 of this part of the article, the reader is introduced to the new design rules for lateral torsional buckling (LTB), which have been significantly expanded in the new edition of the

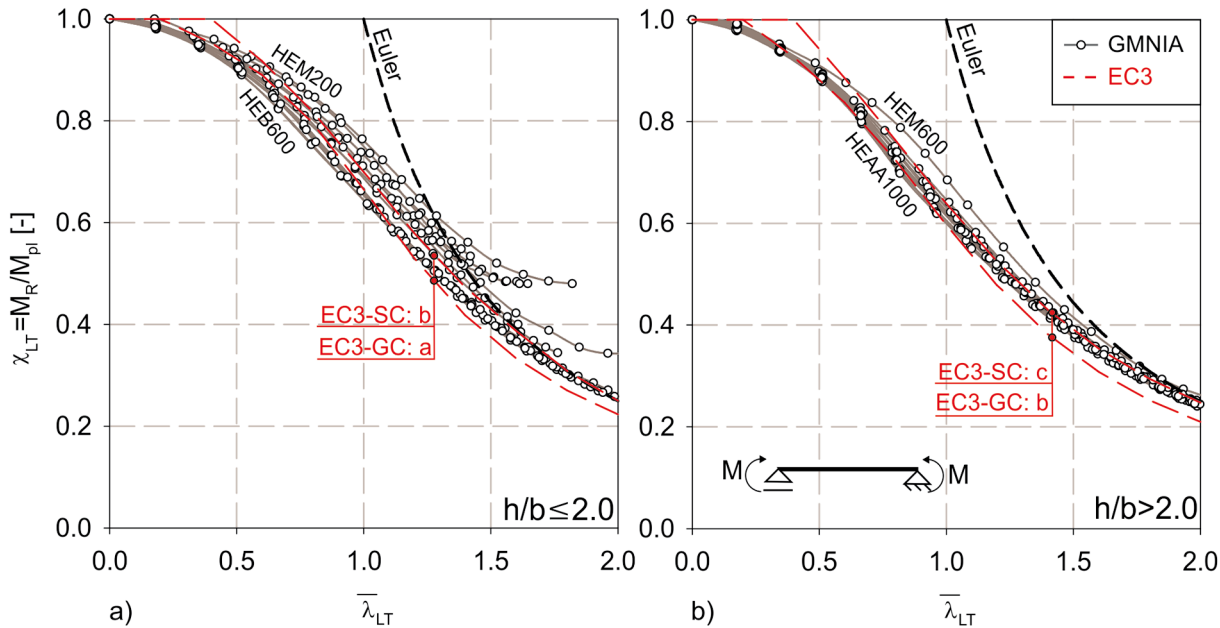
standard: On the one hand, the specific rules for doubly symmetric I- and H-sections have been further improved in terms of their scope, accuracy and safety; on the other, simplified rules have been developed which allow for a clear and practical use of the well-known “equivalent compression flange” concept for a variety of practical cases that are otherwise not easily treated. Subsequently, in section 3, the article illustrates the expansion of beam-column buckling rules to i) mono-symmetric sections and ii) sections loaded in compression, biaxial bending and torsion. Finally, a variety of further, smaller, yet quite relevant changes to member buckling design rules are briefly summarized in section 4. Conclusions relating to the whole two-part article and a further outlook for topics concerning prEN1993-1-1:2020 are given in the fifth and final section.

## 2 New design methods for LTB

### 2.1 General

EN 1993-1-1 currently provides two different sets of LT buckling curves: One set covers “general sections” without pronounced torsional properties, while the other covers “rolled or welded sections” and accounts for their distinct torsional rigidity. Whereas the first set has a plateau length corresponding to merely  $\bar{\lambda}_{LT} = 0.2$  (which is the value also applicable in the case of column buckling), the second set defines the plateau length as  $\bar{\lambda}_{LT} = 0.4$ , which is consistent with the well-confirmed design rules for beams restrained at the compression flange given in Annex BB.3 of EN 1993-1-1 [2]. This second set of LT buckling curves was based on numerical simulations [4] and on beam buckling tests from different sources (e.g. [5], [6]). The question of whether the mechanical accuracy of these curves is appropriate is still controversial. A degree of ambiguity results from the fact that differences are found between the code curves when they are compared with curves determined by numerical FEM simulations using advanced geometrically and materially non-linear analyses with imperfections (GMNIA). Some examples of these discrepancies are given in Fig. 1, which considers the simplest case of doubly symmetric I-sections loaded in uniform bending. As the figure shows, the so-called “general case” rules of EN 1993-1-1, which cover doubly as well as mono-symmetric sections, lead to quite conservative results for many, particularly stockier, sections. The “special case”, which is supposed to cover doubly symmetric rolled sections in particular, is also inaccurate

This is an open access article under the terms of the Creative Commons Attribution License, which permits use, distribution and reproduction in any medium, provided the original work is properly cited.



**Fig. 1** Comparison of GMNIA resistances to lateral torsional buckling (LTB) with code predictions from EN 1993-1-1; comparison of 35 profiles with  $h/b$  values between 0.9 and 3.5; a) sections with  $h/b \leq 2.0$ ; b) sections with  $h/b > 2.0$

for many sections and somewhat unconservative for many sections. As is discussed below, the degree of unconservatism is even more pronounced in the case of other load cases, e.g. with transverse loads.

For these reasons, it was decided to implement newer, more precise and mechanically consistent design rules in section 8 of prEN 1993-1-1:2020 [3].

## 2.2 New buckling reduction factors for doubly symmetric sections

Over the past two decades, knowledge of the specific lateral torsional (LT) buckling behaviour of imperfect members has significantly increased as a result of numerous numerical (GMNIA) simulations using the FE method. The numerical results in Fig. 2 provide an overview of the broad band of numerical buckling curves for I- and H-sections with different torsional properties. Some of them even show a pronounced post-buckling behaviour, which means that for very long beams the limit loads may lie beyond the Euler curve. However, it can be shown that the benefit of this post-buckling resistance has no relevance for practical design, as the corresponding deformations are far above the limits of serviceability.

In addition to this numerical work, progress has also been made on the analytical side, which led to amended and more consistent formulations of “Ayrton-Perry”-type equations for LT buckling. In [7] and [8], formulations for the lateral torsional buckling of I- and H-sections were developed which were based on the concepts originally applied by Ayrton and Perry to design for flexural buckling, i.e. a calibration of a design formulation based on elastic second-order theory and a linear cross-sectional failure criterion through a generalized imperfection defi-

nition. In [8], calibration and validation were finally conducted against a very large series of numerical results and for various load cases. In doing so, a formulation for LTB was obtained analytically which, in most parts, resembles the familiar column buckling formula (which is itself an “Ayrton-Perry” formulation), but includes an additional term  $(\bar{\lambda}_{LT}/\bar{\lambda}_z)^2$  that accounts for and is heavily dependent on the torsional stiffness of the cross-section considered in relation to its weak-axis bending stiffness (Eqs. (7) to (9)). In addition, the formulation derived contains an imperfection term  $\eta = \alpha_{LT} \cdot (\bar{\lambda}_z - 0.2)$ , which was used for calibration in a similar way to the familiar column buckling curves.

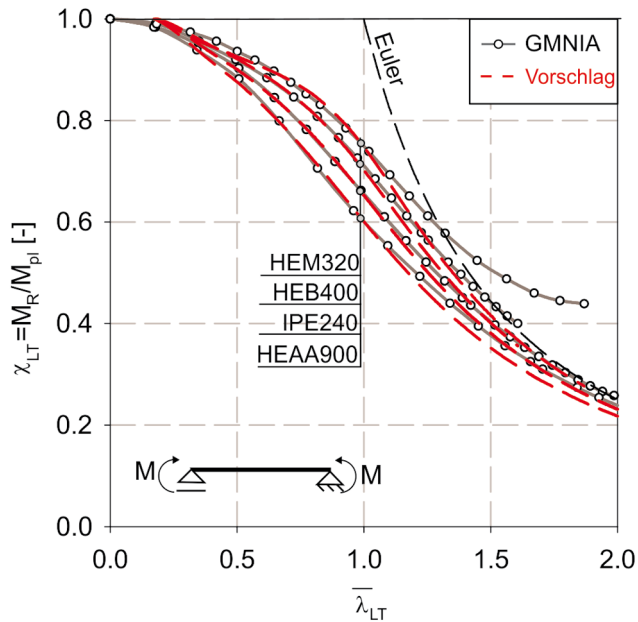
$$\chi_{LT} = \frac{1}{\phi + \sqrt{\phi^2 - \bar{\lambda}_{LT}^2}} \leq 1.0 \quad (1)$$

$$\text{with: } \phi = \frac{1}{2} \cdot \left( 1 + \eta^* + \bar{\lambda}_{LT}^2 \right) \quad (2)$$

$$\eta^* = \eta \cdot \frac{\bar{\lambda}_{LT}^2}{\bar{\lambda}_z^2} = \alpha_{LT} \cdot (\bar{\lambda}_z - 0.2) \cdot \frac{\bar{\lambda}_{LT}^2}{\bar{\lambda}_z^2}; \quad (3)$$

$\alpha_{LT}$  = calibration factor

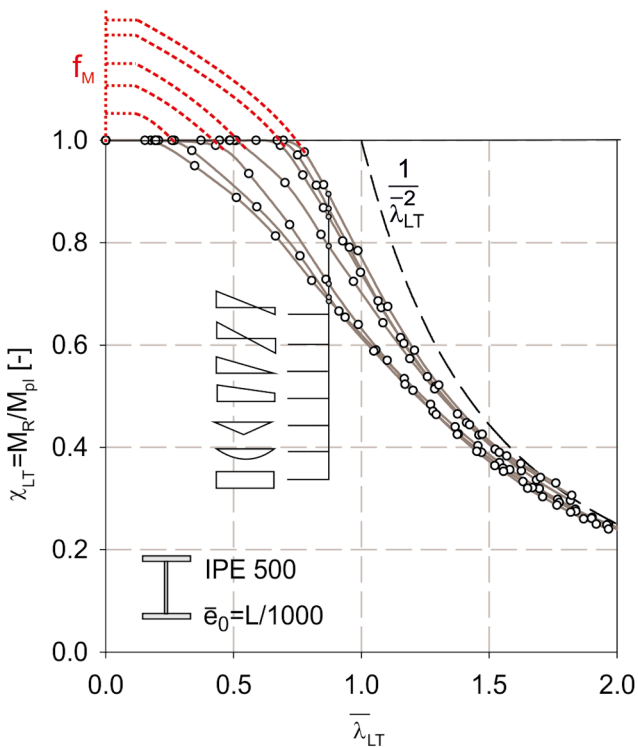
In the calibration of the formula, the different behaviour of I- and H-sections was accounted for by considering the aforementioned factor  $(\bar{\lambda}_{LT}/\bar{\lambda}_z)^2$  and by including an additional factor  $(W_z/W_y)^{0.5}$ , which permitted a much more accurate calibration of the  $\alpha_{LT}$  factor by means of least-square analyses to match the GMNIA buckling curves. It should also be noted that, by introducing this factor, the grouping of the corresponding section shapes no longer follows the previous criterion  $h/b >$  or  $< 2.0$ , but that the section types are now classified in the same way as for flexural buckling, with a classification limit



**Fig. 2** Comparison of GMNIA resistances to lateral torsional buckling (LTB) with the new design rules for LTB of doubly symmetric I- and H-sections in prEN1993-1-1:2020

$h/b = 1.2$ . This emphasizes the consistency of the approach: All sections usually considered to feature the same amplitude of residual stresses are classified into the same group independently of the given buckling mode.

The accuracy of the new concept in terms of buckling reduction factors  $\chi$  is illustrated in Fig. 2. Up to a slender-



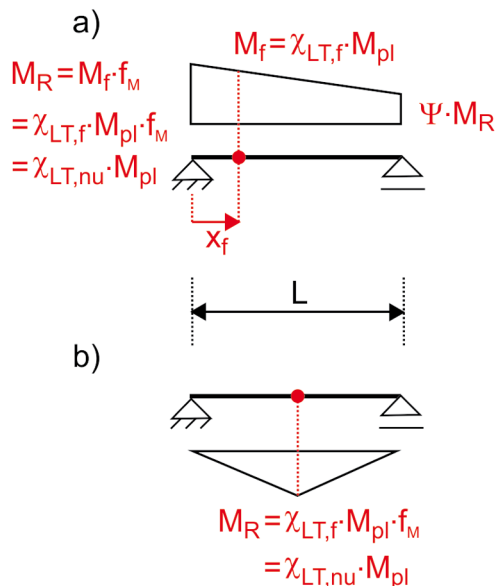
**Fig. 3** Background to factor  $f_M$ , interpreted as an “over-strength” factor when compared with the case with uniform bending moment diagram; a) “over-strength” given by the difference in position between the place with the maximum bending moment (at the boundary) and the position with the maximum influence of the lateral torsional buckling deformations; b) effect of a gradient in the bending moment diagram near the point of maximum LT buckling effects

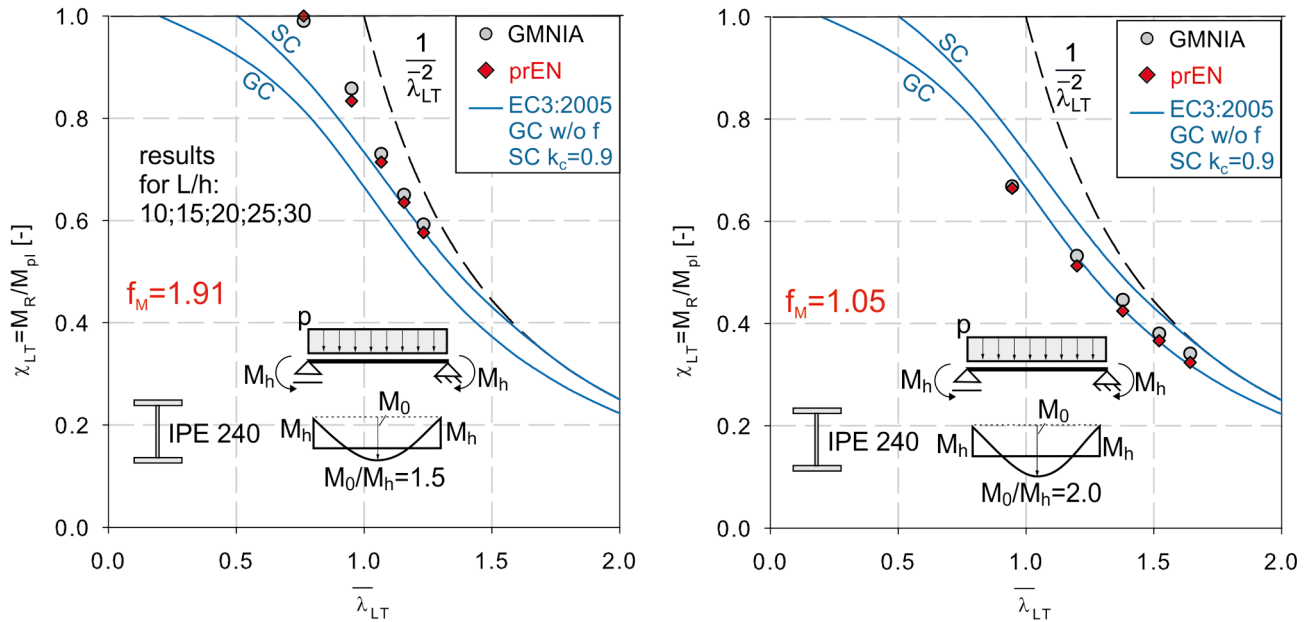
ness  $\bar{\lambda}_{LT} = 1.2$ , the correspondence between design and GMNIA curves is evidently very high. The rather modest deviations on the conservative side – all occurring at higher slenderness only – can be tolerated in light of the fact that I-section beams of lengths that result in values  $\bar{\lambda}_{LT} > 1.2$  when loaded in uniform bending are rarely found in practice. Therefore, the new approach has proved that a consistent derivation means it is possible to establish very accurate design formulae for LT buckling on the basis of the Ayrton-Perry format. However, the prerequisite for this is that the imperfection coefficients are properly calibrated.

Finally, it should be noted that the new design formulation leads to a unique LTB design curve for each section. This needs to be kept in mind when wishing to use tabulated values for the buckling reduction factor  $\chi_{LT}$ .

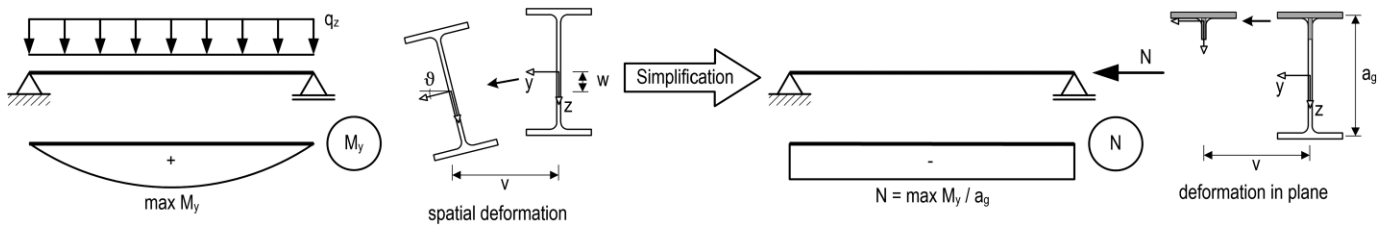
The aforementioned formulation was further expanded in [9] to account for the effect of various bending moment diagrams. This was done through the use of a factor “ $f_M$ ”, which is given for a large set of practically relevant bending moment diagrams in prEN 1993-1-1:2020 and may be seen as an “over-strength” factor for moment diagrams that diverge from the uniform one and mainly accounts for the following two mechanical effects, see Fig. 3:

- a) Firstly, the factor accounts for the fact that the point with the maximum in-plane bending moment may differ significantly from the point on the beam most affected by lateral torsional deformations caused by buckling. Since the design equations only make direct reference





**Fig. 4** Comparison of existing (SC: special case; GC: general case) LTB design rules with the predictions of prEN 1993-1-1:2020 (prEN3) for two typical load cases with transverse load and end moments



**Fig. 5** Simplified lateral torsional buckling design method “buckling of compression flange”

to the point with the maximum bending moment, this causes an increase in the applicable  $\chi_{LT}$  value.

b) In addition, bending moment diagrams with steep gradients, and thus sharp decreases in the moment around the point most affected by LT buckling, provide a degree of support (through a smaller spread of plasticity) that again manifests itself through a higher applicable  $\chi_{LT}$  value.

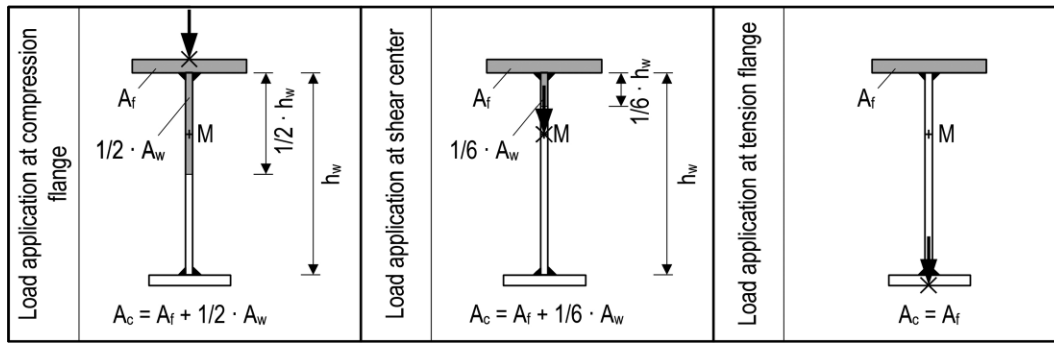
The values of  $f_M$  given in prEN 1993-1-1:2020 significantly expand and improve the bending moment diagrams covered for the design of I- and H-sections for LTB. In the current standard, a similar function is provided by the factor “ $f$ ” in the LT buckling design rules for the “special case” of rolled sections, given in section 6.3.2.3 of EN 1993-1-1. However, the factors and set of rules were found to be significantly inaccurate and often unsafe for certain bending moment diagrams. Fig. 4 illustrates the increase in accuracy when using the new design formulae instead of the existing ones, which can benefit either safety or economy.

### 2.3 The simplified method of the equivalent compression flange

The basic idea behind the simplified method of the equivalent compression flange is to reduce the complex struc-

tural stability behaviour of LT buckling of steel beams with spatial deformations and rotations to the flexural buckling of an equivalent compressed part of the cross-section with horizontal in-plane deformations, see Fig. 5. By neglecting the torsional stiffness of the cross-section and the stabilizing effect of the tension flange, the LT buckling verification can be performed approximately by flexural buckling of the compression flange. This provides an easy-to-use assessment method for engineering practice.

The basic concept of the simplified method has been applied to bridge design since the early 1950s and adapted for other steel structures, e.g. crane runway beams. The existing rules of this concept provided in EN 1993-1-1 [2], section 6.3.2.4, for building structures and EN 1993-2 [10], section 6.3.4.2, for bridge structures are based on the method of the former German standard DIN 18800-2 [11] and its lateral torsional buckling curves. Hence, the current simplified method is neither consistent with the reduction factors of the existing verification rules, i.e. the so-called “general case” according to section 6.3.2.2 and the so-called “specific case” according to section 6.3.2.3, nor the new reduction factors of prEN 1993-1-1:2020 [3], section 8.3.2.3, see section 2.2 of this paper. Moreover, the existing rules have serious shortcomings. On the one hand, it was pointed out in [12] that additional applica-



**Fig. 6** Area of equivalent compression flange for different load positions

tion limits are needed for mono-symmetric sections and girders with load application on the compression flange causing destabilizing effects. For bridge design, on the other hand, an improvement to the rules suggested in [13] was to use buckling curve ‘c’ instead of ‘d’ for welded sections based on the results of residual stress measurements and numerical simulation studies carried out in [14]. The current approach neglects the effect of torsional stiffness and may lead to conservative design results, especially for compact cross-sections with a high  $I_T/I_y$  ratio. This was the starting point for a research project at Ruhr-Universität Bochum and the University of Stuttgart [15]. Within the framework of a comprehensive experimental and theoretical study, the simplified method was further developed on the basis of LT buckling tests and residual stress measurements of doubly and mono-symmetric I-shaped welded sections. A major concern in the further development was to keep the method simple for use in engineering practice and, for instance, to free the user from the need to determine complex cross-sectional values for mono-symmetric cross-sections. Details of the study and the modifications to the simplified method of the equivalent compression flange are given in [16].

The basic idea of the modified simplified method is to determine the lateral torsional buckling resistance  $M_{b,Rd}$  of a steel member as a function of the reduction factor  $\chi_{c,z}$  for flexural buckling of the compression flange:

$$M_{b,Rd} = \chi_{c,z} \cdot W_y \cdot \frac{f_y}{\gamma_{M1}} \quad (4)$$

For the section modulus  $W_y$ , the plastic section modulus  $W_{pl,y}$  may be selected for class 1 and 2 cross-sections. For class 3 cross-sections, however, the elastic modulus  $W_{el,y,min}$  should be used. The latter must be determined with the maximum distance  $z$  from the centre of gravity to the outermost fibre of the cross-section – independent whether it is the tension or the compression flange. For mono-symmetric cross-sections, the verification thus implicitly includes a check of the tension flange. The modified rules do not currently include the application of the method to class 4 cross-sections. The possible extension of the application limit in this respect is currently being evaluated and may be considered in a future draft prEN 1993-2 for steel bridges.

The reduction factor  $\chi_{c,z}$  should be determined taking into account the modified relative slenderness  $\bar{\lambda}_{c,z,mod}$  of the equivalent compression flange (Eq. (5)) and buckling curve ‘c’ for hot-rolled cross-sections and buckling curve ‘d’ for welded cross-sections. In order to determine the modified relative slenderness, the relative slenderness  $\bar{\lambda}_{c,z}$  of the equivalent compression flange should be determined according to Eq. (7).

The cross-sectional axial force capacity and the critical buckling load  $N_{cr,c,z}$  of the equivalent compression flange must be computed as a function of the moment of inertia, which takes into account the corresponding area  $A_c$  of the compression flange according to Fig. 6. This verification procedure enables the effect of the actual point of load application to be considered, i.e. load application at i) the compression flange, ii) the shear centre and iii) the tension flange.

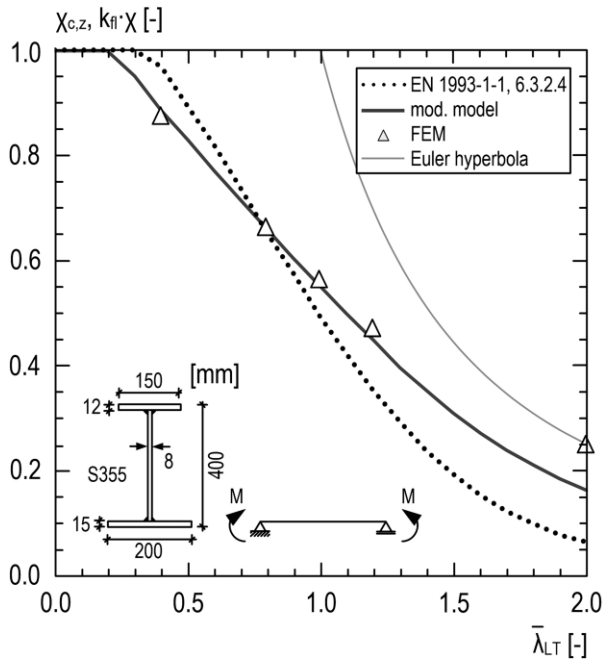
$$\bar{\lambda}_{c,z,mod} = k_c \cdot \beta \cdot \bar{\lambda}_{c,z} \quad (5)$$

with

$$\beta = \sqrt{\frac{0.06 \cdot \frac{h}{t_{max}}}{\bar{\lambda}_{c,z} + \frac{t_{max}}{t_{min}}}} \quad (6)$$

$$\bar{\lambda}_{c,z} = \sqrt{\frac{A_c \cdot f_y}{N_{cr,c,z}}} \quad (7)$$

The next step in the verification procedure is to compute the modified relative slenderness  $\bar{\lambda}_{c,z,mod}$  of the compression flange as a function of the two correction coefficients  $k_c$  and  $\beta$ . Coefficient  $k_c$  takes into account the effect of the bending moment distribution between laterally fixed points and should be determined with Table 8.6 of the draft prEN 1993-1-1:2020. The  $k_c$  values in the new table are consistent with the corresponding values in Table 6.6 of the current EN 1993-1-1. Coefficient  $\beta$  should be computed according to Eq. (6) and enables the influence of the torsional stiffness to be considered by way of the  $h/t_{max}$  ratio. For mono-symmetric cross-sections, the ratio of the flange thicknesses  $t_{max}/t_{min}$  must be considered, too.



**Fig. 7** Comparison of load reduction factors for the modified simplified method of the equivalent compression flange, the old simplified method according to EN 1993-1-1, section 6.3.2.4, and the numerical results

As an example, Fig. 7 compares the results of numerical simulations using the FE method with the design results of the modified simplified method (solid line) and the old simplified method according to section 6.3.2.4 of the current EN 1993-1-1 (dotted line) for a mono-symmetric cross-section. The graph presents the reduction factor  $\chi_{c,z}$  for flexural buckling of the equivalent compression flange about the weak axis (according to prEN 1993-1-1:2020) and the product  $k_{fl}\chi$  of the reduction factor of the equivalent compression flange and the modification factor (according to the current EN 1993-1-1) as a function of the relative slenderness  $\bar{\lambda}_{LT}$  for lateral torsional buckling. The modified method leads to good agreement and provides practitioners with an easily used design method for LT buckling.

### 3 Extension of the scope of stability verifications

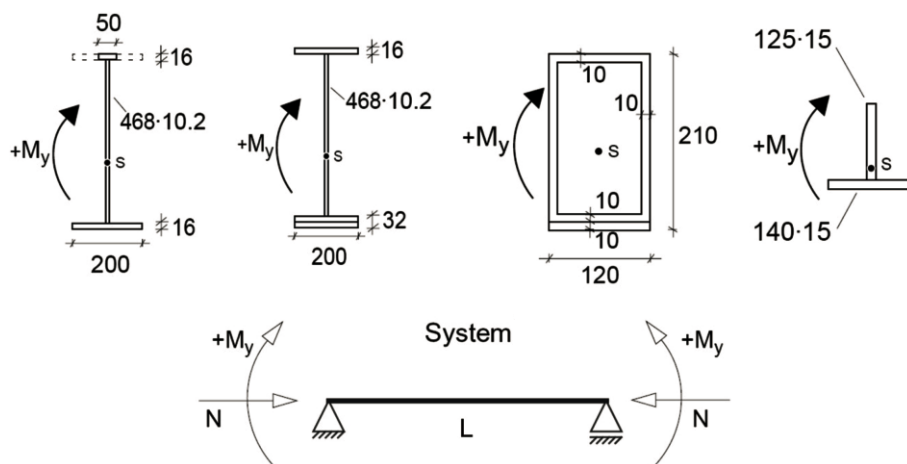
#### 3.1 General

The developments presented in the first part and up to this point in the second part of this article mainly deal with dedicated improvements and expansions to existing analysis and design rules. However, prEN 1993-1-1:2020 also contains a number of additional rules that expand the scope of application of the standard more significantly. In the field of member stability, rules have been added for the design of members with mono-symmetric cross-sections and members subjected to combined bending, compression and torsion, with the detailed specification of the design methods placed in Annex C of the standard. These are described in the following.

#### 3.2 Members with mono-symmetric cross-sections

Annex C.1 of prEN 1993-1-1:2020 contains specific design rules for the buckling checks of members with the mono-symmetric cross-sections shown in Fig. 8. As shown in the figure, the rules apply to mono-symmetric (welded or modified) I- and box sections as well as T-sections when these sections are loaded by compressive forces and/or bending moments acting primarily in a plane parallel with the web ( $M_y$ ). The rules may also be applied in the presence of additional bending moments  $M_z$  about the z-z axis (i.e. moments acting in a plane parallel with the flanges) and are usually more markedly conservative in these cases. The background to these rules is described in detail in [17] and is based on extensive numerical calculations and reliability evaluations.

Owing to the asymmetry of the cross-section about the y-y axis, it is necessary to distinguish between positive and negative values of  $M_{y,Ed}$ , where a positive moment for this purpose being defined as causing compression in the smaller of the two flanges, or in the tip of the web in a T-section.



**Fig. 8** Types of mono-symmetric cross-section covered by the rules in Annex C.1 loaded by compressive forces and bending moments  $M_y$  acting in the plane of the web

The rules included in prEN 1993-1-1:2020 need to account for a number of effects that occur in member buckling scenarios but are not present in doubly symmetric I-sections. These include the following:

- i) In the case of combined compression and bending and member buckling cases dominated by in-plane buckling about y-y (deformations mainly in the x-z plane), the interaction coefficients  $k_{yy}$  specified for doubly symmetric cross-sections in section 8.3.3 of prEN 1993-1-1:2020 could not be confirmed to be sufficiently on the safe side. For this reason, a modification needed to be included in the code.
- ii) For members with open cross-sections that fail in buckling mostly through out-of-plane and torsional deformations, it is necessary to modify the interaction formulae to account for the fact that the failure mode in compression is torsional-flexural buckling instead of flexural buckling about the z-z axis. Thus, the buckling resistance  $N_{b,Rk}$  is determined by applying the torsional-flexural buckling reduction factor  $\chi_{TF}$  to the cross-sectional squash load  $N_R (= A \cdot f_y = N_{pl}$  for class 1 to 3 sections). When this compressive force acts in conjunction with a positive bending moment in accordance with the above definition, the interaction coefficients  $k_{zy}$  of prEN 1993-1-1:2020 describe the beam-column buckling strength quite accurately, provided that the compressive strength  $N_{b,Rk}$  is calculated using the torsional-flexural buckling reduction factor, as described above.  
However, if the compressive force acts in conjunction with a negative bending moment  $M_y$ , the behaviour of the mono-symmetric beam-column changes quite markedly due to the fact that the bending moment relieves the load on the smaller flange. In this case the interaction formula for LT buckling may still be used, but the term relative to the axial force must in this case make use of the weak-axis flexural buckling coefficient  $\chi_z$  in the interaction formula of section 8.3.3 “Uniform members in bending and axial compression”. In addition, for these cases with compression and negative bending moment, it is necessary to verify separately that the axial compressive resistance to torsional-flexural buckling is sufficient to withstand the compressive force acting.
- iii) Finally, the rules in Annex C.1 take into account an additional peculiarity of beam-columns with a mono-symmetric cross-section, i.e. the fact that the “moment diagram coefficients”  $C_m$ , which are used in the interaction formulae of section 8.3.3 in prEN 1993-1-1:2020 (section 6.3.3 of the current EN 1993-1-1) to account for the beneficial effect of non-uniform bending moment diagrams, are no longer directly applicable. The difficulty that arises in the case of mono-symmetric sections mostly stems from the fact that the direction of bending (causing compression in either the larger or the smaller flange) is no longer irrelevant for the use of  $C_m$  factors, unlike for doubly symmetric sections. Thus, the standard values of  $C_m$  are no longer safely applicable, particularly for bending moment dia-

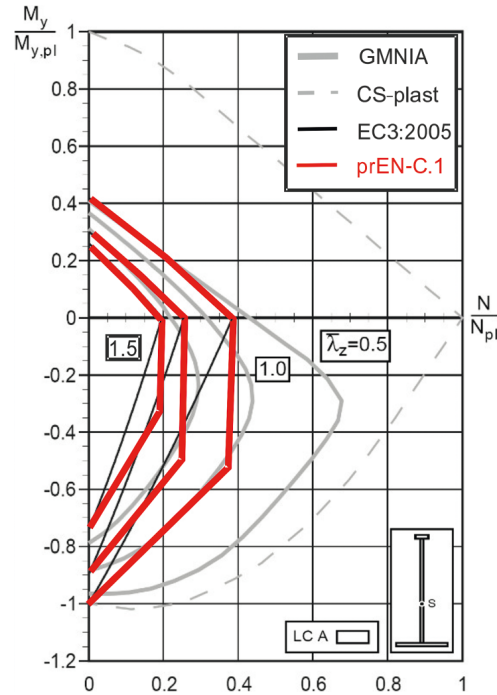


Fig. 9 Comparison of GMNIA results with the new design rules for beam-columns with a mono-symmetric cross-section given in Annex C.1 in prEN 1993-1-1:2020 for a strongly asymmetric welded I-section

grams that change sign. More accurate  $C_m$  coefficients for such cases of bending moment diagrams could theoretically be derived for mono-symmetric sections, but they would heavily depend on the degree of asymmetry of the section and would thus be cumbersome and prone to errors in application. For this reason, it was decided to include only a very simplified regulation in prEN 1993-1-1:2020 in which the  $C_m$  factors do not take account of a change in the sign of the bending moment and must be calculated assuming an equivalent bending moment diagram of the same moment sign along the entire member length. This provision lies on the safe side and is relatively easy to apply, see Fig. 9. If more accuracy is desired, however, the recommendation is to carry out more precise – yet laborious – analyses on the basis of second-order calculations with imperfections, or even GMNIA calculations.

### 3.3 Members in bending, axial compression and torsion

The new Annex C.2 of prEN 1993-1-1:2020 contains a method for assessing the buckling resistance of steel members in bending, compression and torsion. The method is based on the alternative method provided in Annex A of EN 1993-6 [18] for checking the lateral torsional buckling resistance of runway beams in biaxial bending and torsion as well as the findings of German national research project AiF/IGF 19044 N [19] carried out at the University of Stuttgart. The first of these is based on theoretical and experimental investigations [20] within the framework of a German national research project [21]. For the further development of the assessment method, theoretical investigations were carried out in [22] and [23]. The

aim was to remain consistent with the assessment method for checking the buckling resistance of members without scheduled torsion according to EN 1993-1-1, section 6.3.3 (section 8.3.3 of prEN 1993-1-1:2020) and the additional rules for mono-symmetric cross-sections of Annex C.1 of prEN 1993-1-1:2020 described in the previous section.

The new assessment method for members in bending, axial compression and torsion according to Eqs. (8) and (9) extends the common method for the stability verification by including the effect of bi-moments according to [20]. It is possible to use the interaction factors  $k_{ij}$  according to Tables B.1 and B.2 of EN 1993-1-1 (Tables 8.7 and 8.8 of prEN 1993-1-1:2020) for doubly symmetric cross-sections and the new Table C.1 of prEN 1993-1-1:2020 for mono-symmetric cross-sections as well as the equivalent uniform moment factors  $C_m$ . If the sign of the bending moment  $M_{y,Ed}$  changes over the length of the member, the analysis must be performed separately for the maximum values. If the extremal values of the bending moment  $M_{z,Ed}$  are at different positions to those of the maximum  $M_{y,Ed}$  values, the recommendation is to perform the analysis separately for the maximum values with related internal forces and moments. For members of classes 1 and 2, the bending moment resistances  $M_{pl,y}$  and  $M_{pl,z}$  and the bi-moment resistance  $B_{pl}$  can be calculated according to plastic theory. The bending moment resistance  $M_{pl,z}$  and the bi-moment resistance  $B_{pl}$  according to plastic theory are not always reached for a state with full plastic stress distributions. For the plastic cross-sectional capacities, integrating the normal stresses over the cross-section just results in the respective resistance, while all others are zero. For mono-symmetric I-shaped cross-sections, the plastic bending and bi-moment capacities result for a stress state with only partial plastification of the flanges [22]. The computation of the cross-sectional capacities according to plastic theory and associated stress states is usually carried out with the help of software in engineering practice, e.g. the software QST-FZ [24]. For class 3 cross-sections, the cross-sectional capacities according to elastic theory can be used for design. The cross-section of a mono-symmetric section with equal flange thicknesses can be reduced to a doubly symmetric section with the width of the smaller flange when computing the bending moment resistance  $M_{el,z}$  and the bi-moment resistance  $B_{el}$ . Alternatively, the rules for semi-compact cross-sections according to Annex B of prEN 1993-1-1:2020 (see section 3.2 of part 1 [25] of this two-part article) can be applied and partial plastic stress states are used to compute the bending moment resistances. Members with class 4 cross-sections are not covered by Annex C.2.

$$\frac{N_{Ed}}{\chi_y N_{Rk}} + k_{yy} \frac{M_{y,Ed}}{\chi_{LT} M_{y,Rk}} + k_{yz} \frac{M_{z,Ed}}{M_{z,Rk}} + k_w k_{zw} k_\alpha \frac{B_{Ed}}{B_{Rk}} \leq 1.0 \quad (8)$$

$$\frac{N_{Ed}}{\gamma_{M1}} + k_{zy} \frac{M_{y,Ed}}{\chi_{LT} M_{y,Rk}} + k_{zz} \frac{M_{z,Ed}}{M_{z,Rk}} + k_w k_{zw} k_\alpha \frac{B_{Ed}}{B_{Rk}} \leq 1.0 \quad (9)$$

where  $k_{yy}$ ,  $k_{yz}$ ,  $k_{zy}$  and  $k_{zz}$  are the interaction factors,  $\chi_y$  and  $\chi_z$  are the flexural buckling reduction factor,  $\chi_{LT}$  is the reduction factor for lateral torsional buckling and

$$k_w = 0.7 - \frac{0.2 B_{Ed}}{B_{Rk}} \quad (10)$$

$$k_{zw} = 1.0 - \frac{M_{z,Ed}}{M_{z,Rk}} \quad (11)$$

$$k_\alpha = \frac{1}{1 - \frac{M_{y,Ed}}{M_{cr}}} \quad (12)$$

Furthermore, some limitations need to be considered when applying the assessment method of Annex C.2. The method only applies to simply supported members with a uniform cross-section. It covers rolled and welded cross-sections with both equal flanges (doubly symmetric I-shaped cross-sections) and unequal flanges (mono-symmetric I-shaped cross-sections). For the latter, the ratio of the moment of inertia for the minor axis (z-z axis) of the smaller flange to the entire section must be  $\geq 1/6$  and  $\leq 0.5$ . These limits cover the scope of the theoretical studies carried out for the establishment of the method and prevent its application to T-shaped cross-sections with only one flange or mono-symmetric I-sections with one very narrow and one significantly wider flange. The structural behaviour of such cross-sections in bending, axial compression and torsion can differ markedly from the behaviour of typical mono-symmetric I-sections.

The value of the bi-moment  $B_{Ed}$  is also limited. It should not exceed 30% of the bi-moment resistance  $B_{Rk}/\gamma_{M1}$ . This limit ensures the consistency of the method with the verification of the buckling resistance of members without scheduled torsion according to EN 1993-1-1, section 6.3.3 (section 8.3.3 of prEN 1993-1-1:2020) and at the same time allows resistances according to plastic theory of torsionally weak I-sections to be taken into account, especially IPE sections and equivalent welded mono- and doubly symmetric cross-sections. However, such cross-sections are not very suitable for use in torsion.

The following simplification has a great benefit for engineering practice. The influence of the bi-moment on the structural stability behaviour of a simple member can be neglected if the product of the amplifier  $k_\alpha$  and the bi-moment ratio  $B_{Ed}/(B_{Rk}/\gamma_{M1})$  does not exceed 0.07. In this



case the assessment method can lead to design results unconservative by up to 5% at the level of the load amplifiers. Alternatively, a conservative rule can be applied for small bi-moment values. If the bi-moment ratio  $B_{Ed}/(B_{Rk}/\gamma_{M1})$  is  $\leq 0.035$ , its effect may also be neglected.

In addition to the structural stability check, sufficient resistance of the cross-section must be verified. As a simplification, the linear plastic interaction equation (Eq. (13)) can be used for members with class 1 and 2 cross-sections.

$$\frac{N_{Ed}}{N_{Rd}} + \frac{M_{y,Ed}}{M_{y,Rd}} + \frac{M_{z,Ed}}{M_{z,Rd}} + \frac{B_{Ed}}{B_{Rd}} \leq 1.0 \quad (13)$$

Alternatively, non-linear plastic interactions can also be used, e.g. the partial internal forces method [22],[26]. This can result in internal forces and moments that exceed the bending moment and bi-moment capacities according to plastic theory. As already mentioned above, mono-symmetric I-sections are only partially plasticized when their plastic capacities are reached. However, the consideration of cross-section resistances above the plastic capacities requires that the respective other internal forces and moments are necessarily available. The analyses and checks must be performed for the locations of extreme internal forces and moments generating normal stresses and shear stresses. Therefore, is usually also necessary to verify the cross-sectional resistance at the supports for simply supported members.

## 4 Further improvements and innovations

### 4.1 General

In addition to the main changes discussed in the previous sections of this paper, prEN 1993-1-1:2020 contains a significant number of smaller, yet often equally important modifications and improvements to and expansion of the scope of applicability of the current design rules. Some of these are briefly summarized in the following. They concern simplified rules regarding load introduction without stiffeners, verification rules for elliptical hollow sections and buckling curves for heavy sections and angles as well as revised buckling curves for grade S460. The scope of and background to these rules will be briefly described below.

### 4.2 Local load introduction without stiffeners

The introduction of concentrated transverse loads into the webs of hot-rolled or welded beams and girders without stiffeners is a common detailing solution that needs a proper design check, particularly in building structures. Practical design checks for this detailing solution were thus included in national standards that preceded the introduction of the Eurocodes. The current design rules in Eurocode 3 deal with the introduction of transverse loads

into unstiffened webs through the rules in EN 1993-1-5 for welded (bridge) plate girders, and through some dedicated rules in EN 1993-1-8 for the detailing of unstiffened beam-to-column moment-resistant connections. These rules were simplified and generalized to the common cases found in beams and girders in buildings in [27], thus once again allowing for a simple design check of this common detail. The results of this study were adapted and implemented in prEN 1993-1-1:2020.

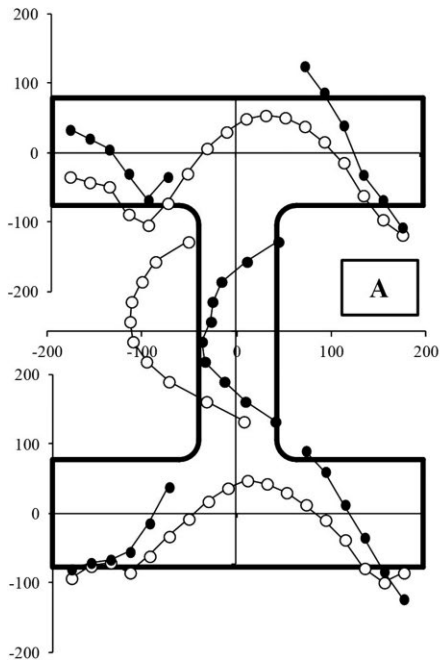
### 4.3 Circular and elliptical hollow sections

One of the innovations in the steel construction industry that took hold over the course of the last decade was the development and application of elliptical hollow sections (EHS). Although they share many features of the behaviour of circular hollow sections (CHS), they also require some additional considerations that are more familiar in rectangular hollow section (RHS) design, such as the existence of weak and strong bending axes as well as the related, stronger dependence on the direction and degree of bending during the classification of the cross-section. The behaviour of EHS has been studied in various publications (e.g. [28]). These studies led to the development of dedicated classification limits for EHS as well as to – quite importantly – the development and validation of simple and practical formulae for determining the effective cross-sectional properties  $A_{eff}$  and  $W_{eff}$  for EHS and – as a “special case” – CHS. These effective properties are particularly useful for the practical determination of the cross-sectional strength of EHS and CHS members with locally slender (class 4) cross-sections. A definition of  $A_{eff}$  and  $W_{eff}$  for CHS (and EHS) was missing in EN 1993-1-1, thus often requiring designers to carry out a local buckling check in accordance with the shell structures design code EN 1993-1-6, which is a cumbersome and inaccurate approach for fabricated hollow sections. For this reason, the findings regarding  $A_{eff}$  and  $W_{eff}$  values for CHS and EHS have been included in prEN 1993-1-1:2020.

In addition, it is clarified in prEN 1993-1-1:2020 that the rules for designing members in compression and bending for global buckling given in section 8.3.3 (section 6.3.3 in EN 1993-1-1) apply to all types of standard hollow section, including CHS and EHS.

### 4.4 Buckling curves for heavy sections

For rolled sections with depth-to-width ratio  $h/b > 1.2$ , buckling curves are currently not specified for flange thicknesses  $t_f > 100$  mm. However, such heavy sections are available nowadays. The present gap in Table 6.2 of EN 1993-1-1 hampers the use of these innovative European products. A research project was carried out at Eindhoven University of Technology in The Netherlands to measure the residual stresses (Fig. 10) and carry out finite element analyses. Details of the study, including geo-



**Fig. 10** Residual stress measurements for an HD 400 × 1202 section [31]

metric values and material properties, are reported in [29], [30], [31], [32]. Based on this research, the buckling curve selection table has now been supplemented for heavy sections with depth-to-width ratio  $h/b > 1.2$  and flange thicknesses  $t_f > 100$  mm. It was further shown that a distinction between  $40 \text{ mm} < t_f \leq 100 \text{ mm}$  and  $t_f > 100 \text{ mm}$  could not be justified, resulting in the simplification to only two classes for flange thickness:  $t_f \leq 40 \text{ mm}$  and  $t_f > 40 \text{ mm}$  for  $h/b > 1.2$ , see Tab. 1.

#### 4.5 Buckling curves for angles

When designing an I-section, a distinction is made between hot-rolled and welded sections. This is not so for the design of angle sections, also called L-sections. From the figure for L-sections in Table 6.2 of the current version of EN 1993-1-1, it is obvious that only hot-rolled sections are meant. However, the text within Table 6.2 of EN 1993-1-1 mentions “L-sections”, not specifying whether rolled or welded sections are meant. In the past, angles were almost always rolled. However, nowadays, due to the fact that very heavy thick-wall rolled angles are available, there is competition between rolled and welded angles. Owing to the aforementioned unclear content of Table 6.2 in EN 1993-1-1, the same buckling curve is currently used for both types. However, the choice of buckling curve also depends on the residual stresses in the section, which may be far more unfavourable for welded angles than for rolled angles. So unconservative designs for welded angles can ensue if the buckling curve for rolled angles is used. As residual stresses in grade S460 rolled angles are relatively low and therefore less detrimental, the buckling curve for S460 can be more favourable than for lower steel grades. This advantage should now be considered because S460 angles are currently

available. For these reasons, the following modifications are proposed [33]:

- For hot-rolled L-sections, use buckling curve ‘a’ for steel grade S460 and buckling curve ‘b’ for steel grades S235 to S420.
- For welded L-sections with flange thickness  $t_f \leq 40 \text{ mm}$ , use buckling curve ‘c’ for all steel grades.

This leads to an adjusted buckling curve selection Tab. 1, which is the buckling curve selection Table 8.3 in prEN 1993-1-1:2020. The figures in Tab. 1 for angles now also state that the buckling curves apply to equal and unequal leg angles.

In order to arrive at the buckling curves of Tab. 1 for angles, a research project was carried out for hot-rolled and welded L-sections by Liège University in Belgium [34] and the University of Ljubljana in Slovenia [35] and [36]. The primary goal was to arrive at realistic buckling curves by means of residual stress measurements and finite element analyses.

Residual stresses were measured in large hot-rolled and welded angle sections and numerical simulations performed for members in compression made from such sections. Each university measured the residual stresses on eight steel angle sections. Six of these sections were hot-rolled, two of them welded. The L-sections were welded as shown in Fig. 11. The sectioning method was used to measure residual stresses. This method is based on the principle that internal stresses are relieved by cutting the specimen into many strips with a smaller cross-section. The measured residual stress values were statistically analysed and several distributions of residual stresses included in a numerical model to obtain the buckling resistanc-

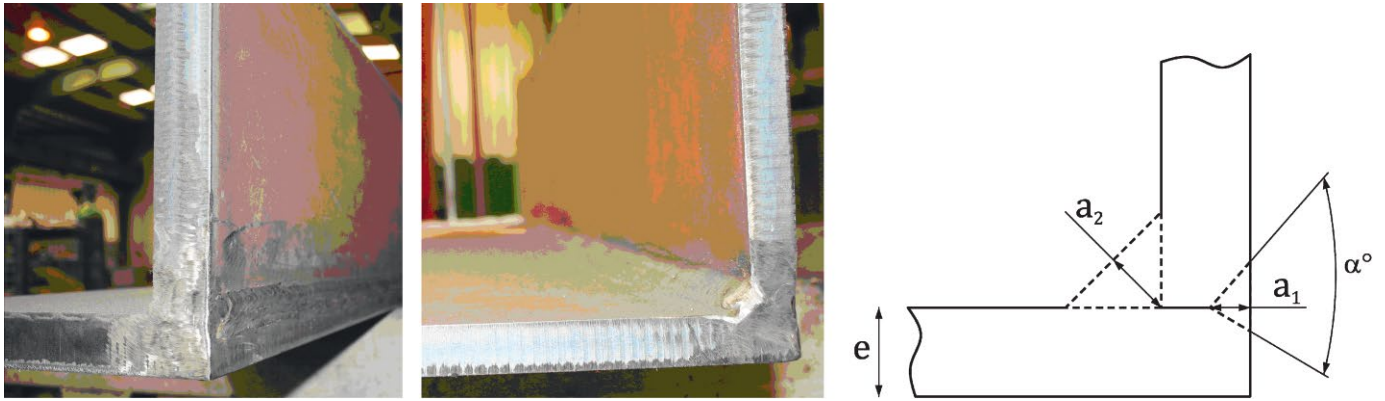


Fig. 11 Welded L-sections

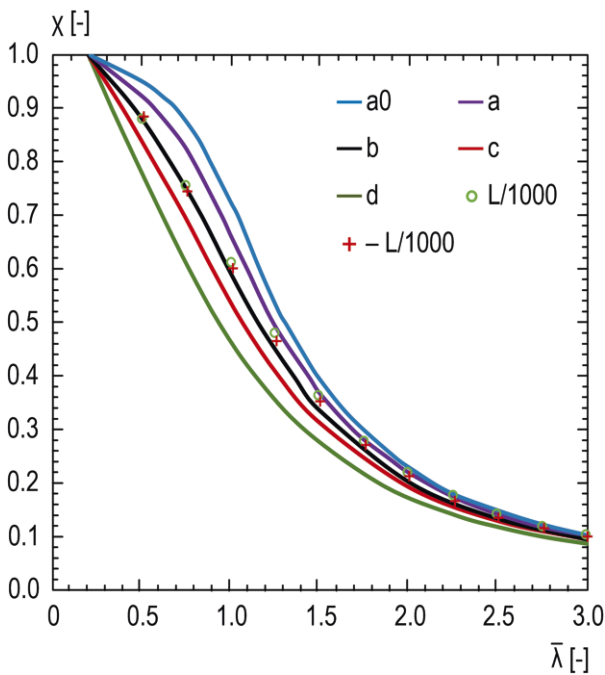


Fig. 12 Numerical simulations for rolled angles in grade S235 compared with the buckling curves

es of angle sections. Geometrical imperfections were also taken into account. This resulted in the new buckling curves for steel angle sections. The elastic-plastic flexural buckling response of hot-rolled L-sections is best represented by buckling curve ‘a’ for steel grades S420 and S460 and by buckling curve ‘b’ for steel grades S235 to S355. However, in order to retain the existing steel grade subdivision of Table 6.2 of EN 1993-1-1, it was decided to adopt curve ‘a’ for S460 hot-rolled sections only. As an example, Fig. 12 shows the result for rolled angles in grade S235, confirming buckling curve ‘b’.

#### 4.6 Buckling curves for rolled I- and H- sections in grade S460

The buckling curve selection Table 6.2 in the current version of EN 1993-1-1 prescribes the same buckling curve with respect to weak- and strong-axis buckling for S460

and a depth-to-width ratio  $h/b > 1.2$  for all flange thicknesses  $t_f$  and for  $h/b \leq 1.2$  for  $t_f \leq 100$  mm. For the other steel grades (S235 to S420) this is different: Buckling about the z-z axis is more unfavourable than buckling about the y-y axis (except for heavy sections with  $h/b \leq 1.2$  for  $t_f > 100$  mm). Various numerical investigations ([37], [38], [39]) show that this classification is inconsistent and that the safety level is not uniform for all cases in the buckling curve selection Table 6.2 of EN 1993-1-1, which therefore must be changed as indicated in Tab. 1.

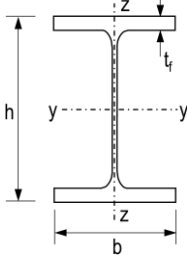
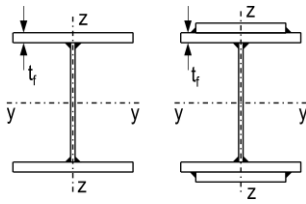

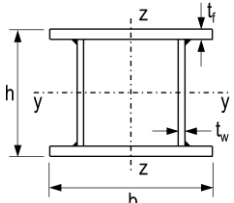
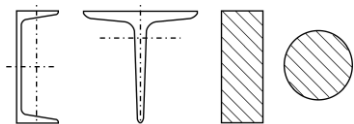
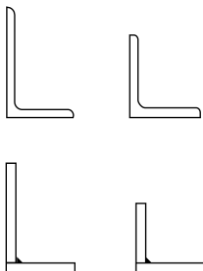
These modifications result in consistent safety levels throughout the buckling curve selection table and the proposed buckling curves may be used in combination with the current  $\gamma_{M1}$  value.

Ultimate resistance calculations for flexural buckling of some rolled sections, taking into account residual stresses, geometrical imperfections and plastic zones along the column length, are presented in [38]. The results for S460 show that the relative ultimate resistance (ultimate resistance divided by full plastic resistance), using the present Table 6.2 of EN 1993-1-1 and calculated based on nominal values of  $f_y$ , yields values less than 1 (see Fig. 13), in contrast to the results for other steel grades.

A parametric study for the evaluation of rules for flexural buckling of prismatic columns is presented in [39]. This parametric study covers several slenderness ranges, residual stress levels, yield stresses and cross-section shapes such that it is possible to conduct a thorough evaluation of the members covered by the stability design rules analysed using advanced non-linear numerical simulations. In particular, a great number (about 7300) of ultimate resistance calculations for flexural buckling about the minor z-z axis were undertaken. These show that the level of safety is consistent across the various types of I- and H-shaped cross-sections and steel grades except for S460 and minor-axis buckling. The main results are shown in Fig. 14.

On the basis of the work reported in [38] and [39], the buckling curves for I- and H-sections in grade S460 have been modified to the ones mentioned in Tab. 1.

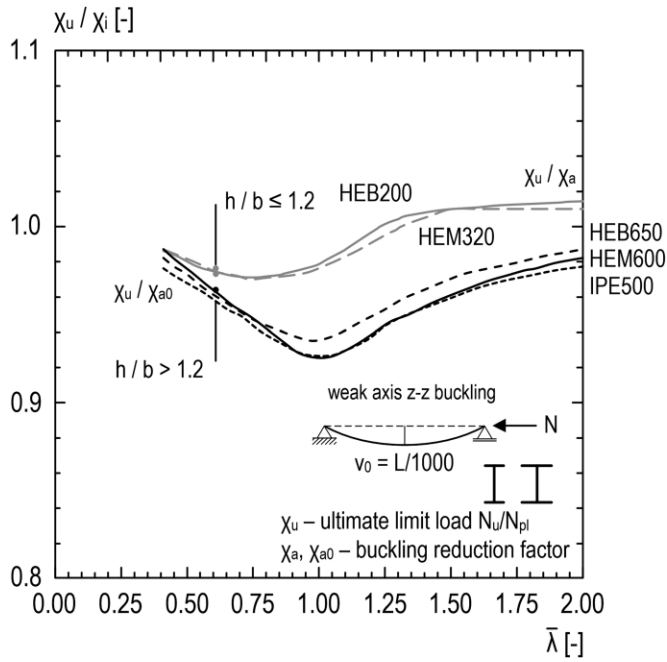
**Tab. 1** Buckling curve selection Table 8.3 in prEN 1993-1-1:2020

Cross-section	Limits	Buckling about axis	Buckling curve		
			S 235 S 275 S 355 S 420	S 460 to S 700	
Rolled sections 	$h/b > 1.2$	$t_f \leq 40$ mm	y - y	a	a <sub>0</sub>
			z - z	b	a
	$h/b \leq 1.2$	$t_f > 40$ mm	y - y	b	a
			z - z	c	b
		$t_f \leq 100$ mm	y - y	b	a
			z - z	c	b
$t_f > 100$ mm	y - y	d	c		
	z - z	d	c		
Welded I-sections 	$t_f \leq 40$ mm	y - y	b	b	
		z - z	c	c	
	$t_f > 40$ mm	y - y	c	c	
		z - z	d	d	
Hollow sections 	hot-finished	any	a	a <sub>0</sub>	
	cold-finished	any	c	c	
Welded box sections 	generally (except as below)	any	b	b	
	thick welds: $a > 0.5 t_f$ and $b/t_f < 30$ , and $h/t_w < 30$	any	c	c	
U-, T- and solid sections 		any	c	c	
L-sections 	Rolled sections	any	b	a	
	Welded sections $t_f \leq 40$ mm	any	c	c	

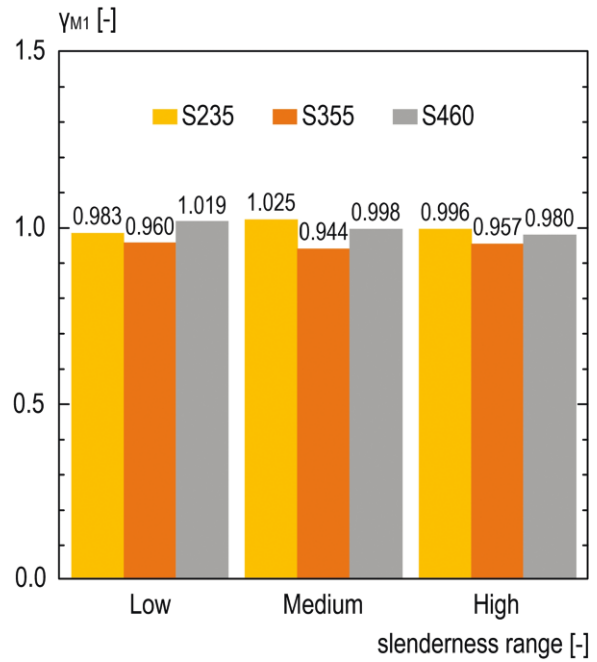
**5 Conclusions and future steps**

This two-part article has presented the developments in structural member verification that will be implemented in the upcoming revision of Part 1-1 of EN 1993. These developments are currently published in the form of a

pre-standard, prEN 1993-1-1:2020 [3], one of the second generation of Eurocodes that will be reviewed by the National Mirror Groups over the course of the next few years. The first part of this article, published in the preceding issue of this journal, was mostly dedicated to the general background to European Commission Mandate



**Fig. 13** Results of resistance calculations for different rolled sections in grade S460



**Fig. 14** Normalized partial safety factor  $\gamma_{M1}$  for different slenderness ranges: low (0.5 to 0.8), medium (0.8 to 1.5) and high (1.5 to 2.5) for current buckling curves

M/515 for the evolution of the Eurocodes and to the changes in prEN 1993-1-1:2020 that concern material grades and partial factors, cross-sectional classification and checks as well as structural analyses. This second part of the article was mostly dedicated to developments pertaining to member buckling design rules.

The intention of the article is to familiarize the future users of this standard with the main structural and technical changes. These changes aim to improve ease-of-use especially in view of clarity, harmonize the rules both within Eurocode 3 and with related standards and integrate new findings from research and technical developments. This will help to improve structural designs and enhance the economic efficiency of steel structures.

The developments presented in this two-part article significantly contribute to achieving the overall objectives of the second generation of the Eurocodes. Eurocode prEN 1993-1-1:2020 for the structural design of steel structures is aimed at the well-educated structural engineer and offers practical design approaches. Moreover, this state-of-the-art standard allows and promotes responsible innovation.

**References**

[1] CEN/TC 250 (2013) *Response to Mandate M/515 (Mandate for amending existing Eurocodes and extending the scope of structural Eurocodes) "Towards a second generation of EN Eurocodes"*, Brussels, CEN-TC250\_N993.  
 [2] EN 1993-1-1 (May 2005) *Eurocode 3: Design of steel structures – Part 1-1: General rules and rules for buildings*, CEN, Brussels.

In addition to Part 1-1, all the other parts of Eurocode 3 will also be revised. The completion of Part 1-8 will take place shortly; Parts 1-3, 1-5, 1-6, 1-7 on structural stability as well as Part 1-2 for fire design are part of phase 2 of Mandate M/515. These parts are currently still being revised by their project teams. However, consolidated drafts will be published soon. These parts of Eurocode 3 as well as the general and application parts of Eurocode 3, which will be revised in phases 3 and 4 of Mandate M/515, will provide practitioners with a future-oriented standard for structural steel design. This enormous task is being undertaken by a large number of experts throughout Europe who are involved in 22 SC3 Working Groups and 13 SC3 Project Teams, see section 1 of the first part of this article. They are supported by members from industry, consulting offices and academia who, through the National Mirror Groups and numerous informal and formal enquiries, comment on the drafts and thus influence the developments of Eurocode 3. These procedures enhance the transparency and, ultimately, the acceptance of the new Eurocode, hopefully leading to a fruitful implementation.

[3] prEN 1993-1-1:2020 (Dec 2019) *Eurocode 3: Design of steel structures – Part 1-1: General rules and rules for buildings*, Doc. CEN-TC250-SC3\_N3023.  
 [4] Greiner, R.; Kaim, P. (2001) *Comparison of LT-buckling design curves with test results*, ECCS TC8, report, 23 Apr 2001, European Convention for Constructional Steelwork (2001), Brussels.

- [5] Byfield, M. P.; Nethercot, D. A. (1998) *An analysis of the true bending strength of steel beams* in: Proc. of Institution of Civil Engineers, Structures & Buildings 128, pp. 188–197.
- [6] CEC (1988) ENV background doc. 5.03, Commission of the European Community, Brussels.
- [7] Stangenberg, H. (2007) *Zum Bauteilnachweis offener, stabilitätsgefährdeter Stahlbauprofile unter Einbeziehung seitlicher Beanspruchungen und Torsion*, Dissertation, RWTH Aachen.
- [8] Taras, A.; Greiner, R. (2010) *New design curves for lateral torsional buckling – Proposal based on a consistent derivation* in: Journal of Constructional Steel Research 70, Elsevier London/Amsterdam.
- [9] Taras, A. (2011) *Contribution to the Development of Consistent Stability Design Rules for Steel Members*. Institute for Steel Structures & Shell Structures, Graz University of Technology, Vol. 16, Graz.
- [10] EN 1993-2 (2006) Eurocode 3: *Design of steel structures – Part 2: Steel Bridges*, CEN, Brussels.
- [11] DIN 18800-2 (2008) *Stahlbauten, Teil 2: Stabilitätsfälle, Knicken von Stäben und Stabwerken*.
- [12] Beyer, A.; Bureau, A. (2019) *Simplified method for lateral torsional buckling of beams with lateral restraints* in: Steel Construction 12, No. 4, pp. 318–326.
- [13] Davaine, L. (2018) Meeting presentation for SC3/WG13 Steel Bridges in 2018, CEN-TC250-SC3-WG13\_N57, p. 24, 15 Feb 2018.
- [14] Thiébaud, R.; Lebet, J.-P. (2014) *Resistance to LTB of Steel Bridge Girders* in: Eurosteel 2014, Naples, Italy; Landolfo, R.; Mazzolani, F. M. (eds.), p. 759–760.
- [15] Knobloch, M.; Kuhlmann, U. (2020) *Simplified method for lateral torsional buckling – consistent model for welded beams at ambient and elevated temperatures*. Project AiF/IGF: 19439 N, 1 Apr 2017 – 31 Mar 2020
- [16] Schaper, L.; Jörg, F.; Winkler, R.; Kuhlmann, U.; Knobloch, M. (2019) *The simplified method of the equivalent compression flange* in: Steel Construction 12, No. 4, pp. 264–277.
- [17] Taras, A.; Gonzalez Puig, M.; Unterweger, H. (2013) *Behaviour and design of members with monosymmetric cross-section* in: Proc. of ICE – Structures & Buildings, 166, No. 8, ICE publishing, London,
- [18] EN 1993-6 (2007) Eurocode 3: *Design of steel structures – Part 6: Crane supporting structures*, CEN, Brussels.
- [19] Kuhlmann, U. (2019) *Interaktionsbeziehungen für Normalkraft, Biegemomente und Torsion: Harmonisierung und Ergänzung der Stabilitätsnachweise für Stäbe mit Standard-Walzprofilen*. Project AiF/IGF: 19044 N, 1 Feb 2016 – 30 Apr 2019.
- [20] Lindner, J.; Glitsch, T. (2004) *Vereinfachter Nachweis für I- und U-Träger – beansprucht durch doppelte Biegung und Torsion* in: Stahlbau 73, No. 9, pp. 704–715.
- [21] Kindmann, R.; Lindner, J.; Sedlacek, G.; Wolf, C.; Beier, J.; Glitsch, T.; et al. (2004) *Untersuchungen zum Einfluss der Torsionseffekte auf die Querschnittstragfähigkeit und Bauteiltragfähigkeit von Stahlprofilen*. Research report P 554, Forschungsvereinigung Stahlanwendungen e.V., Düsseldorf.
- [22] Bours, A.-L.; Winkler, R.; Knobloch, M. (2019) *Ergänzende Untersuchungen zum Tragverhalten einfachsymmetrischer I-Querschnitte unter Biegung, Druck und Torsion* in: Stahlbau 88, No. 9, pp. 836–850.
- [23] Winkler, R.; Walter, A.; Knobloch, M. (2018) *Zum Stabilitätsnachweis von Stahlbauteilen aus einfach- und doppelt-symmetrischen I-Querschnitten unter Biegung, Druck und Torsion* in: Stahlbau 87, No. 5, pp. 476–490.
- [24] RUBStahl (2019) *Teaching/learning program for studies/training*. Ruhr-Universität Bochum, Chair of Steel, Lightweight & Composite Structures.
- [25] Knobloch, M.; Bureau, A.; Kuhlmann, U.; Simões da Silva, Luis; Snijder, Hubertus H.; Taras, A.; Bours, A.-L.; Jörg, F. (2020) *Structural member stability verification in the new Part 1-1 of the second generation of Eurocode 3 – Part 1: Evolution of Eurocodes, background to partial factors, cross-section classification and structural analysis* in: Steel Construction 13, No. 2, pp. 98–113.
- [26] Winkler, R.; Kindmann, R.; Knobloch, M. (2019) *Assessment of the plastic capacity of I-shaped cross-sections according to the partial internal forces method* in: Engineering Structures 191, pp. 740–751.
- [27] Unterweger, H.; Taras, A. (2019) *Steifenlose Krafteinleitung bei Biegeträgern – Vorschlag einer vereinfachten Eurocode-konformen Nachweisführung* in: Stahlbau 84, No. 6, pp. 435–448.
- [28] Gardner, L.; Chan, T. M.: (2007) *Cross-section classification of elliptical hollow sections* in: Steel and Composite Structures 7, No. 3, pp. 185–200.
- [29] Cajot, L. G.; Snijder, H. H. (2014) *Buckling curves for heavy wide flange rolled sections*, Doc. CEN-TC250-SC3\_N2031.
- [30] Snijder, H. H.; Cajot, L. G.; Popa, N.; Spoorenberg, R. C. (2014) *Buckling curves for heavy wide flange steel columns* in: Romanian Journal of Technical Sciences – Applied Mechanics 59, Nos. 1–2, pp. 178–204.
- [31] Spoorenberg, R. C.; Snijder, H. H.; Cajot, L. G.; May, M. S. (2013) *Experimental investigation on residual stresses in heavy wide flange QST steel sections* in: Journal of Constructional Steel Research 89, pp. 63–74.
- [32] Spoorenberg, R. C.; Snijder, H. H.; Cajot, L. G.; Popa, N. (2014) *Buckling curves for heavy wide flange QST columns based on statistical evaluation* in: Journal of Constructional Steel Research 101, pp. 280–289.
- [33] Cajot, L. G. (2014) *Buckling curves for L-sections*, Doc. CEN-TC250-SC3\_N2017.
- [34] Zhang, L.; Jaspert, J. P. (2013) *Stability of members in compression made of large hot-rolled and welded angles*, Université de Liege.
- [35] Beg, D.; Rejec, K.; Sinur, F. (2013) *Determination of buckling curves for large angle profiles considering different steel grades and different residual stress patterns*, University of Ljubljana, Faculty of Civil & Geodetic Engineering.
- [36] Beg, D.; Može, P.; Rejec, K.; Sinur, F. (2013) *Report on the residual stress measurements and numerical determination of buckling curves for large angle profiles*, University of Ljubljana, Faculty of Civil & Geodetic Engineering, 2013.
- [37] Lindner, J.; Simoes da Silva, L. (2015) *Classification of rolled I-Profiles fabricated in steel grade S460 within Table 6.2 of EN 1993-1-1*, Doc. CEN-TC250-SC3\_N2164.
- [38] Lindner, J. (2015) *Classification of rolled I-profiles fabricated in steel grade S460 within table 6.2 of EN 1993-1-1, Rev. 3*, Report to Working Group 1.
- [39] Simoes da Silva, L.; Tankova, T.; Marques, L.; Rebelo, C. (2015) *Safety assessment of EC3 stability design rules for flexural buckling of columns*, v40, Report to Evolution Group 1.

## Authors

Prof. Dr. sc. techn. Markus Knobloch (corresponding author)  
markus.knobloch@rub.de  
Ruhr-Universität Bochum  
Chair of Steel, Lightweight & Composite Structures  
Universitätsstr. 150  
44801 Bochum, Germany

Alain Bureau  
abureau@cticm.com  
Centre Technique Industriel de la Construction Métallique (CTICM)  
Research & Valorization Dept.  
Immeuble Apollo  
91193 Saint-Aubin, France

Prof. Dr.-Ing. Ulrike Kuhlmann  
ulrike.kuhlmann@ke.uni-stuttgart.de  
University of Stuttgart  
Institute of Structural Design  
Pfaffenwaldring 7  
70569 Stuttgart, Germany

Prof. Luís Simões da Silva  
luisss@dec.uc.pt  
University of Coimbra  
Institute for Sustainability & Innovation in Structural Engineering  
Rua Luís Reis Santos – Pólo II  
3030-788 Coimbra, Portugal

Prof. ir Hubertus. H. Snijder  
h.h.snijder@tue.nl  
Eindhoven University of Technology  
Dept. of the Built Environment  
P.O. Box 513  
5600 MB Eindhoven, The Netherlands

Prof. Dr. techn. Andreas Taras  
taras@ibk.baug.ethz.ch  
ETH Zurich  
Chair of Steel & Composite Structures  
Stefano-Franscini-Platz 5  
8093 Zurich, Switzerland

Anna-Lena Bours, MSc  
anna-lena.bours@rub.de  
Ruhr-Universität Bochum  
Chair of Steel, Lightweight & Composite Structures  
Universitätsstr. 150  
44801 Bochum, Germany

Fabian Jörg, MSc  
fabian.joerg@ke.uni-stuttgart.de  
University of Stuttgart  
Institute of Structural Design  
Pfaffenwaldring 7  
70569 Stuttgart, Germany

## How to Cite this Paper

Knobloch, M.; Bureau, A.; Kuhlmann, U.; da Silva, L. S.; Snijder, H.; Taras, A.; Bours, A.-L.; Jörg, F. (2020) *Structural member stability verification in the new Part 1-1 of the second generation of Eurocode 3 – Part 2: Member buckling design rules and further innovations*. Steel Construction 13, No. 3, pp. 208–222.  
<https://doi.org/10.1002/stco.202000027>

This paper has been peer reviewed. Submitted: 15. April 2020; accepted: 1. May 2020.